Photocrosslinking Detects a Compact, Active Structure of the Hammerhead Ribozyme†

Joyce E. Heckman, Dominic Lambert, and John M. Burke*

Department of Microbiology and Molecular Genetics, University of Vermont, 95 Carrigan Drive, 220 Stafford Hall, Burlington, Vermont 05405

Received October 4, 2004; Revised Manuscript Received December 20, 2004

ABSTRACT: The hammerhead ribozyme has been intensively studied for approximately 15 years, but its cleavage mechanism is not yet understood. Crystal structures reveal a Y-shaped molecule in which the cleavage site is not ideally aligned for an S_N2 reaction and no RNA functional groups are positioned appropriately to perform the roles of acid and base or other functions in the catalysis. If the ribozyme folds to a more compact structure in the transition state, it probably does so only transiently. We have used photocrosslinking as a tool to trap hammerhead ribozyme−substrate complexes in various stages of folding. Results suggest that the two substrate residues flanking the cleavage site approach and stack upon two guanosines (G8 and G12) in domain 2, moving 10−15 Å closer to domain 2 than they appear in the crystal structure. Most crosslinks obtained with the nucleotide analogues positioned in the ribozyme core are catalytically inactive; however, one cobalt(III) hexaammine-dependent crosslink of an unmodified ribozyme retains catalytic activity and confirms the close stacking of cleavage site residue C17 with nucleotide G8 in domain 2. These findings suggest that residues involved in the chemistry of hammerhead catalysis are likely located in that region containing G8 and G12.

The hammerhead ribozyme is a member of a class of small catalytic RNAs (including the hairpin, hepatitis *δ*, Neurospora VS, and newly discovered bacterial GlmS ribozyme) (*1*), which carry out reversible cleavage of RNA, generating products containing 2′,3′-cyclic phosphate and 5′-OH termini. The hammerhead cleavage reaction results in inversion of the configuration of the phosphate and thus is presumed to occur by deprotonation of the 2′-OH group, followed by in-line S_N2 attack of the 2′-O^- upon the phosphate (*2*, *3*).

The cleavage rate of hammerhead ribozymes increases in log-linear fashion with increasing pH, and thus, early investigations centered on the likelihood of a catalytic magnesium acting at the cleavage site (*4*). However, it was discovered that the cleavage reaction could be mediated (albeit at around a 10−40-fold reduced rate) by high concentrations of monovalent ions (*5*−*7*). These findings suggest that divalent ions serve primarily to promote folding of the ribozyme. A directly coordinated divalent ion might play a role in driving formation of the active ribozyme structure and/or in providing a favorable electrostatic environment at the active site. On the other hand, the activity of the ribozyme in monovalent ions suggests that a general acid−base mechanism may be utilized in the reaction and that important roles in the catalysis may be carried out by functional groups of the RNA itself.

Crystal structures have been reported for the hammerhead ribozyme (*8*, *9*) as well as for two other members of this class, the hairpin ribozyme (*10*) and the hepatitis *δ* ribozyme (*11*). In the case of the hairpin ribozyme, the crystal structure shows two domains of the RNA docked together, with the guanosine 3′ of the cleavage site (G+1) engaged in a base pair with C25 in the other domain. This relationship helps to twist the backbone at the cleavage site into an alignment permissive for an S_N2 reaction. Moreover, the tightly docked structure places functional groups of two nucleotides (G8 and A38) close enough to the cleavable linkage to have potential roles in the reaction, and biochemical results have confirmed the importance of the Watson−Crick face of G8 in the reaction (*12*).

The hepatitis *δ* ribozyme crystal structure, although produced with a self-cleaved product, also shows a very tightly packed region around the cleavage site, with a cytidine residue positioned close enough to the cleaved linkage to help catalyze the reaction (*11*). Again, biochemical results suggest that this cytidine may have a role in facilitating the reaction (*13*, *14*).

The crystal structures of the hammerhead ribozyme do not permit such happy correlations with biochemical studies. The crystals from two different constructs (*8*, *9*) reveal a Y-shaped molecule with all three branches of the Y in one plane. The crystal lattice in each case is stabilized by intermolecular interactions between a GNRA loop (*15*) on one molecule and a GNRA loop receptor sequence in the stem of a neighboring molecule. The cleavable linkage of the substrate is not aligned appropriately for an S_N2 reaction, and it is not closely approached by functional groups of ribozyme residues that could help mediate the reaction. Additionally,

† This work is supported by Grant GM65552 to J.M.B. from the National Institutes of Health.

* To whom correspondence should be addressed: Department of Microbiology and Molecular Genetics, University of Vermont, 95 Carrigan Drive, 220 Stafford Hall, Burlington, VT 05405. Telephone: (802) 656-8503. Fax: (802) 656-5172. E-mail: John.Burke@uvm.edu.

10.1021/bi047858b CCC: $30.25
Published on Web 02/18/2005

the crystal structure offers no obvious explanations for many of the biochemical observations that have accumulated over many years of hammerhead studies. The most frequently quoted discrepancy arises from the importance of G5 in functional studies. Any alterations to the Watson−Crick face of G5 cause severe decreases in activity, usually dropping the reaction rate by a factor of about 10^3 (*16*). However, in the crystal structure, G5 is part of a "U-turn" motif (*17*) and its base is solvent-exposed, making no close interactions with any other residues of the substrate or ribozyme (*4*).

In addition to crystallographic analyses, mutational studies, and extensive nucleotide analogue substitution studies (*4*, *18*), the hammerhead has been subjected to analysis by fluorescence resonance energy transfer (FRET) (*19*), transient electric birefringence (TEB) (*20*), backbone protection (*21*), nondenaturing gel electrophoresis (*22*), and other methods. Results of these studies seem to suggest that the global structure of the ribozyme in solution is very similar to the Y-shaped molecule observed in the crystals, except for hints that helices I and II may approach each other more closely in some constructs (*20*). Thus, investigators are faced with a conundrum: if the crystal structure represents the "resting" or basic fold of the hammerhead ribozyme, then some structural rearrangement seems to be required for the molecule to access the transition state. However, no method to date has identified an alternative structure more consistent with biochemical findings. The putative rearrangement could be a very subtle one (*23*), or it might lead to a transient active conformation that is very hard to observe within the total molecular population.

We have addressed this question by doing an extensive set of photocrosslinking studies on the hammerhead ribozyme−substrate complex, using nucleotide analogue crosslinking agents incorporated at specific positions into chemically synthesized RNA molecules, then activated by long-wavelength (312 nm) UV light. This approach has the potential to identify nucleotide stacking relationships in the RNA structure, even those that occur only transiently during accession of the transition state. For example, a nucleotide such as G5, which is not tightly stacked in the crystal structure, might move into a more congested region and stack closely upon another nucleotide in the active structure. A crosslinking agent at position 5 might therefore mediate a crosslink only upon accessing that active structure.

This paper describes the acquisition and analysis of a large set of photocrosslinks, primarily those covalently linking ribozyme residues to the substrate in HH16 (Figure 1). It also describes crosslinks obtained in two other hammerhead constructs without nucleotide analogues, using short-wavelength (254 nm) UV light. These results strongly suggest that the two nucleotides flanking the cleavable linkage in the hammerhead substrate access an alternative conformation in which they are intimately stacked with guanosines 8 and 12 in domain 2 of the ribozyme. In most cases, the various crosslinked species failed to show retention of definitive catalytic activity while still crosslinked, making it difficult to identify folding constraints diagnostic of the active structure. Strikingly, a photocrosslink in HH∝1 (Figure 1) mediated by cobalt hexaammine confirms the close approach of the cleavage site nucleotides to G8 in domain 2, and the crosslinked species can catalyze the cleavage reaction while still covalently linked. This validates the structural information represented by the crosslinks and implies that the active structure of the hammerhead ribozyme moves the cleavage site closely into domain 2. Once there, residues G8 and G12 may be close enough to participate in the chemistry of the cleavage reaction. In fact, in another effort, biochemical studies of these residues and G5 show that G8 and G12 do appear to play roles in the reaction chemistry and may be largely responsible for the log-linear pH-rate profile of the hammerhead (*24*).

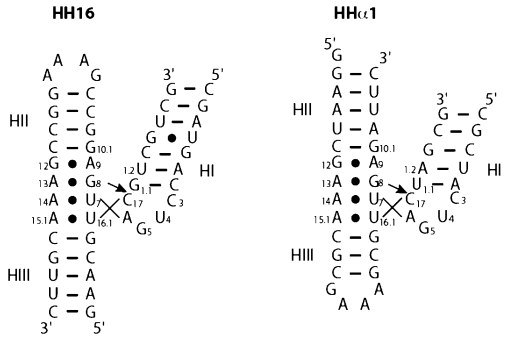

FIGURE 1: Minimal hammerhead ribozyme constructs HH16 (a slightly shortened version used in this work) and HH∝1. Cleavage sites are marked with arrows, and important residues of the ribozyme core and cleavage site are numbered. The connectivities of the two constructs vary such that the substrate of HH16 is a separate strand from the ribozyme, whereas the cleavage site of HH∝1 is in the long strand of the ribozyme, leaving the 5′ portion of the substrate sequence still as part of the long strand.

MATERIALS AND METHODS

Preparation of RNA Oligonucleotides. All RNAs utilized in this study were produced by solid-phase synthesis on an Applied Biosystems 392 DNA/RNA Synthesizer. They were deprotected and purified as described previously (*25*). Phosphoramidites, including those for nucleotide analogues, were purchased from Glen Research and Chemgenes. Oligonucleotides containing 6-thio-2′-deoxyguanosine and 4-thio-2′-deoxyuridine were deprotected by a protocol provided by Glen Research.

Photocrosslinking. Ribozymes or substrates containing nucleotide analogue crosslinking agents were assembled with one strand 5′-^{32}P-labeled and the other strand in excess (0.2−2 μM), in 50 mM tris(hydroxymethyl)aminomethane hydrochloride (Tris)-HCl[1] at pH 8 [or 50 mM 3-(*N*-morpholino)propanesulfonic acid (MOPS) at pH 6.5] and preincubated at 37 °C for 10 min. Samples were placed at room temperature, adjusted to 20 mM $MgCl_2$, and exposed to a 312 nm hand-held UV lamp (with a polystyrene plate to screen shorter wavelengths) at a 1 cm distance for 5 min. Loading solution containing 90% formamide and 0.1 mg/mL tRNA was added to denature the sample and minimize free-radical damage. Samples were fractionated by electrophoresis on 20% acrylamide gels containing 8 M urea. Bands were eluted, extracted with chloroform, precipitated with ethanol, dried, dissolved in 50 μL of H_2O, and desalted on Centri-Sep columns (Princeton Separations) before analysis.

Crosslinking of unmodified native hammerhead and HH∝1 in cobalt hexaammine [$Co(NH_3)_6^{3+}$] was carried out as described for ribozymes with crosslinking agents, except that

[1] Abbreviations: Tris, tris(hydroxymethyl)aminomethane hydrochloride; MOPS, 3-(*N*-morpholino)propanesulfonic acid.

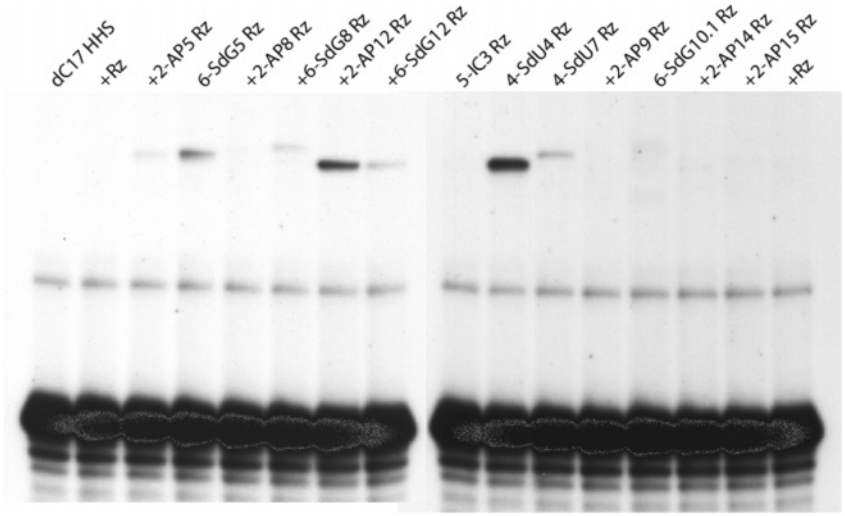

FIGURE 2: Photocrosslinking of HH16 with photoreactive nucleobase analogues incorporated at the indicated sites (i.e., 2AP8Rz indicates 2-aminopurine at core position 8 of HH16). Ribozymes were assembled for this survey with noncleavable (dC17) 5′-labeled substrate strand in 50 mM Tris-HCl at pH 8 and 20 mM $MgCl_2$, subjected to 312 nm UV light for 5 min, and then analyzed by denaturing 20% PAGE. Uncrosslinked end-labeled substrate is at the bottom of the pattern. The lower band present in each lane is an internal substrate crosslink, and interstrand ribozyme−substrate crosslinks are the slower-moving bands. Note that the unsubstituted HH16 ribozyme (+Rz) yields no interstrand crosslinks under these conditions.

the RNA was unmodified and 10 mM $Co(NH_3)_6Cl_3$ was used in placed of $MgCl_2$.

Sequence Analysis of Crosslinked Strands. Crosslinks were localized by subjecting purified end-labeled crosslinked strands to partial digestion with ribonuclease T1 and partial hydrolysis with alkali (*26*, *27*). Uncrosslinked end-labeled strands were digested similarly to provide control patterns. Treated samples were fractionated on 20% denaturing polyacrylamide gels and visualized by autoradiography.

Cleavage Activity Assays for Crosslinked Species. Purified, desalted crosslinked ribozyme complexes were incubated in 50 mM Tris-HCl at pH 8, 20−30 mM $MgCl_2$, and 0.1 mM aurin tricarboxylic acid (ATA, a ribonuclease inhibitor that does not inhibit ribozyme cleavage) at 37 °C for 2−3 h. Aliquots were removed at 0 and 2 h or at more frequent intervals and analyzed by denaturing gel electrophoresis. In most cases, duplicate crosslinks with the opposite strand labeled were also tested to help differentiate cleavage in the crosslinked species from cleavage following reversal of the crosslink bond. In the case of the active $Co(NH_3)_6^{3+}$-mediated HH∝1 crosslink, a negative control for cleavage was produced by crosslinking and analyzing products from a 2′-deoxy-C17 long strand. This crosslink was identical to that produced with a cleavable strand, except that the crosslinked species was not cleaved.

RESULTS

Incorporation of Nucleotide Analogue Photocrosslinking Agents into Positions of Interest in the HH16 Ribozyme and Substrate. Over the course of these experiments, five different crosslinking agents commercially available as nucleotide phosphoramidites were incorporated singly at each of 10 positions in the ribozyme core of HH16 and at 2 positions in the substrate strand. 6-thio-2′-deoxyguanosine (6-S-dG) was inserted into positions 5, 8, 10.1, and 12 in the ribozyme and position 1.1 of the substrate. 4-thio-2′-deoxyuridine (4-S-dU) was used at positions 4 and 7 of the ribozyme and 16.1 of the substrate. 8-bromo-guanosine (8-BrG) was incorporated at ribozyme positions 5, 8, and 12, and 5-iodocytosine (5-IC) was incorporated at 3. Finally, 2-aminopurine (2-AP) was incorporated at ribozyme positions 5, 8, and 12, plus 9, 14, and 15.1.

Because these nucleotide analogues absorb ultraviolet light at longer wavelengths than the four normal nucleotides, RNAs containing them were activated with 312 nm UV light and tested for formation of interstrand (modified ribozyme to 5′-end-labeled substrate or vice-versa) crosslinks, under conditions that permit folding and cleavage for HH16. Figure 2 shows a survey experiment testing 13 derivatized HH16 ribozymes and the unmodified control ribozyme against noncleavable (2′-deoxy-C17) 5′-^{32}P-labeled substrate for crosslinking with 312 nm UV light. Denaturing polyacrylamide gel electrophoresis (PAGE) resolves crosslinked species as slow-moving bands. Under these conditions, the unmodified ribozyme and several of the derivatized species yielded no crosslinks. Crosslink formation by all of the nucleotide analogues used here should be detected only if the modified nucleotide stacks closely with a base from the other strand of the ribozyme−substrate complex when it is exposed to UV light. When photocrosslink products of this type have been characterized in chemical studies, they sometimes show rearrangement of either the modified nucleotide or target base, but they generate a covalent linkage between the two bases (*28*). Nearly all of the observed crosslinked species were single bands that could be mapped to unique target sites. Only 6-S-dG10.1 yielded multiple faint crosslink bands, which were not analyzed further.

Mapping of Photocrosslink Target Sites in HH16 Substrate and Ribozyme. Derivatized HH16 ribozymes or substrates that yielded interstrand crosslinks were then used in preparative reactions with cleavable end-labeled substrates or end-labeled unmodified ribozymes, respectively. Crosslinked species were cut from gels, eluted, concentrated by ethanol precipitation, and then desalted. The target sites of the crosslinks were identified by RNA sequence analysis (*26*). End-labeled RNAs were partially digested at 50 °C with T1

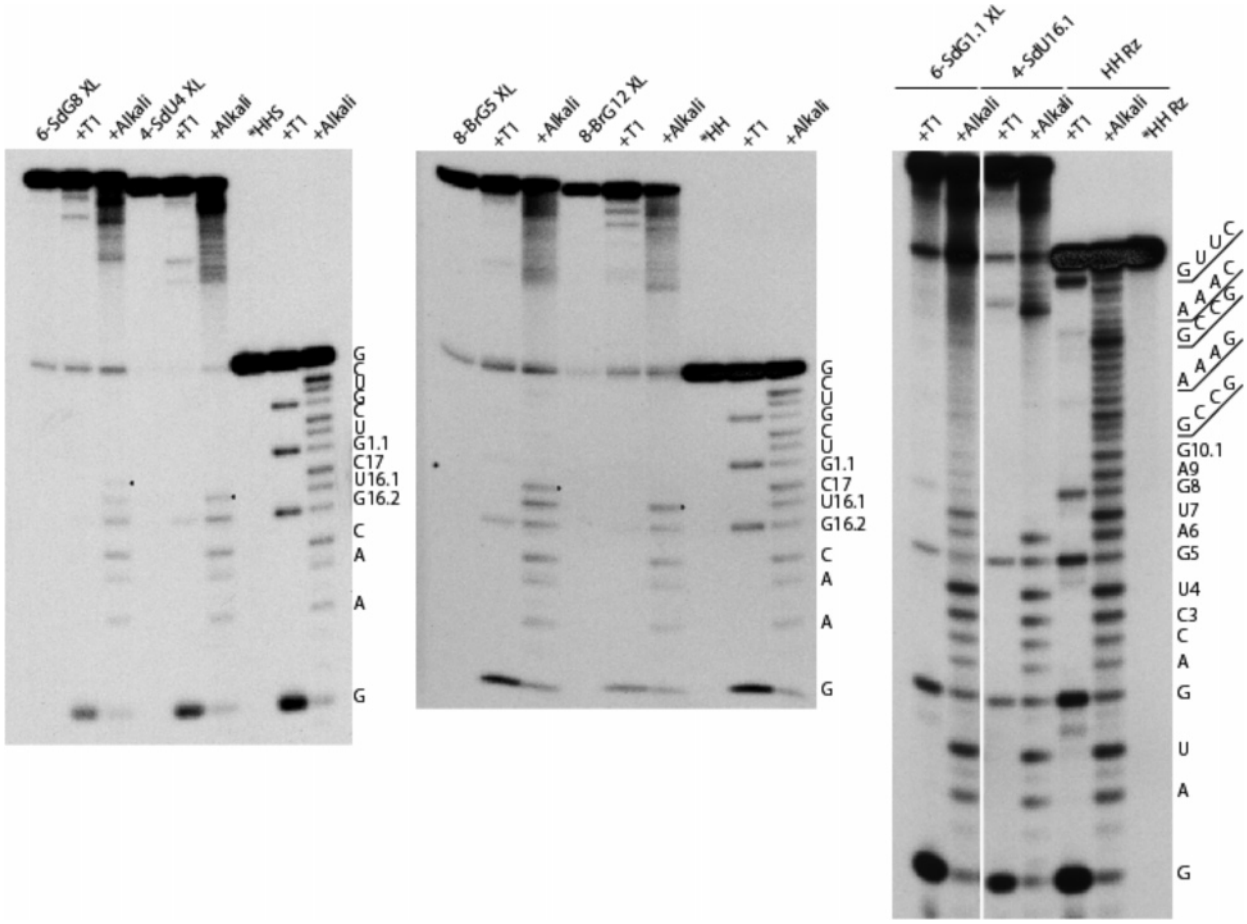

FIGURE 3: RNA sequence analysis of end-labeled crosslinked and control strands to identify target sites of crosslinking agents incorporated at different positions in HH16 ribozyme (first two gels) and HH16 substrate (gel on the right). Lanes are marked with the identity of the nucleotide analogue used, followed by its position in the molecule (6-SdG8XL indicates a crosslink from 6-thio-2′-deoxyguanosine at position 8 of HH16). Lanes marked "+T1" and "+Alkali" are patterns of the same sample subjected to partial hydrolysis with T1 ribonuclease or alkali, as described in the Materials and Methods. Control patterns of uncrosslinked labeled strands are at the right side of each gel. The last band in the +Alkali lane of each crosslinked sample identifies the nucleotide 5′ of the photocrosslink target. Thus, for the crosslink from 8-BrG5 (middle gel), the last band is C17, and the crosslink targets G1.1. For 8-BrG12, the last band is U16.1 and the crosslink targets C17. The gel on the right shows analysis of crosslinks made with nucleotide analogues in HH16 substrate (positions 1.1 and 16.1) to 5′-end-labeled HH16 ribozyme. Note that the crosslinking of G8 from 6-S-dG1.1 is a reciprocal crosslink to one shown in the gel on the left.

ribonuclease or alkali and then analyzed by denaturing PAGE alongside patterns of control uncrosslinked strands. Because the crosslink produces a branch point on the end-labeled RNA strand, sequence analysis yields a normal ladder pattern from the 5′-labeled end to the nucleotide involved in the crosslink, where the pattern ceases. Figure 3 shows sequencing gels analyzing several of the crosslinks exemplified in Figure 2.

Table 1 summarizes results from numerous preparative photocrosslinking reactions and analyses, listing the ribozyme construct used, the position from which the crosslink was obtained, the modified nucleotide used (if any), the crosslink target, the UV wavelength, and multivalent ions included. Crosslinks obtained from G8 without crosslinking agents will be discussed below.

Table 1 shows that the hammerhead substrate could be crosslinked to the ribozyme with crosslinking agents placed at ribozyme core positions 4, 5, 7, 8, and 12. The crosslink targets in the substrate all map to C17, G (or U) 1.1, or U1.2, flanking the cleavage site. This suggests that the crosslinks at least represent assembled ribozyme−substrate complexes at some stage of folding, because the remaining substrate

Table 1: Summary of HH16 and HH∝1 Crosslinking Results, Describing Constructs, Crosslinking Agents, Wavelengths, and Metal Ions Used to Obtain Photocrosslinks[a]

	XL agent	target	wavelength (nm)	metal	ribozyme
ribozyme nt					
4	4-thio-dU4	C17	312	Mg^{2+}	HH16
5	6-thio-dG5	G1.1	312	Mg^{2+}	HH16
5	8-bromo-G5	G1.1	312	Mg^{2+}	HH16
5	none	U1.2 + G1.1	312	$Co(NH_3)_6^{3+}$	HH16
7	4-thio-dU7	C17	312	Mg^{2+}	HH16
8	6-thio-dG8	G1.1	312	Mg^{2+}	HH16
8	none	U1.1	254	Mg^{2+}	HHα1
8	none	*C17 + (U1.1)	312	$Co(NH_3)_6^{3+}$	HHα1
12	6-thio-dG	C17 + (G1.1)	312	Mg^{2+}	HH16
12	8-bromo-G	C17	312	Mg^{2+}	HH16
12	2-AP	C17	312	Mg^{2+}	HH16
substrate nt					
G1.1	6-thio-dG1.1	G8	312	Mg^{2+}	HH16
16.1	4-thio-dU16.1	U7	312	Mg^{2+}	HH16

[a] Target sites were identified by RNA sequence analysis as described. An asterisk indicates that the crosslinked species retains catalytic activity. Agents and ribozyme positions that yielded no crosslinks or amounts insufficient for analysis include 2-AP at 8, 9, 14, and 15; 5-Iodo-C at 3; 6-S-dG at 10.1; and 8-Br-G at 8.

residues would be expected to be involved in helical stems and would not be free to stack on nucleotides from the ribozyme core. Figure 6 shows the photocrosslinks superimposed upon the crystal structure model of the hammerhead complex.

The photocrosslinks targeting C17 from 4-thio-2′-deoxyuridine at positions 4 and 7 are fairly easily explained within the constraints of the crystal structure, as is the crosslink from 4-S-dU16.1 of the substrate strand to U7. On the other hand, crosslinking agents placed at the positions of three important guanosines in the ribozyme core, G5, G8, and G12, yield crosslinks suggestive of stacking relationships much more compact and intimate than those represented in the crystal structure. 6-S-dG, 8-BrG, and 2-AP at position 12 in the ribozyme all crosslink to substrate residue C17, just 5′ of the cleavage site (6-S-dG12 also results in about 5−10% of the crosslink mapping to G1.1, just 3′ of the cleavage site). When 6-S-dG was placed at position 8 in the ribozyme, its crosslink target was G1.1. A reciprocal version of this crosslink was obtained when 6-S-dG1.1 in the substrate yielded a crosslink to G8 of the ribozyme. Finally, 6-S-dG and 8-BrG placed at ribozyme position 5 result in crosslinks to G1.1.

None of these crosslinks from positions 12, 8, and 5 correlates with potential stacking relationships in the ribozyme crystal structure. The crosslinked residues are separated by 12−16 Å distances in each case (Figure 6). If they represent a real configuration of the ribozyme, it would be one in which the cleavable linkage of the substrate is moved very close to domain 2, allowing stacking of C17 upon G12 and G1.1 upon G8. This would most likely also entail a change to the "U-turn" motif, perhaps moving G5 closer to its crosslinking target, G1.1.

This set of crosslinks obviously represents more than one conformation of the hammerhead ribozyme−substrate complex. All were obtained under conditions that permitted assembly of the complex and cleavage of the substrate. Some of the nucleotide analogues decreased cleavage activity at certain positions, but none rendered the ribozyme completely inactive. 6-S-dG, for instance, incorporated at position 12 resulted in nearly wild-type cleavage activity. At positions 5 and 8, it inhibited activity rather severely, consistent with reports that 2′-deoxy-G decreases cleavage activity when present at position 5 or 8 of the hammerhead (*16*). In an effort to assess possible folding artifacts because of the 2′-deoxy residues, we incorporated 8-BrG (ribo) at positions 5, 8, and 12. 8-BrG is a weak crosslinking agent, but it yielded enough crosslinking product from positions 5 and 12 to confirm that the targets were the same as those obtained with 6-S-dG at those positions.

Hammerhead ∝1 Ribozyme and a Variant of a Natural Ribozyme Each Yield Spontaneous G8-Py1.1 Crosslinks when Exposed to Short Wavelength UV Light. In the course of backbone protection studies of several hammerhead constructs (*21*), it was noted that free-radical reactions produced apparent crosslinks in HH∝1 (Hampel and Burke, unpublished results) but not in HH16 nor in HH6, the construct used in crystallization studies (*9*). Exposure of these three hammerhead variants to 254 nm light under cleavage conditions confirmed this observation, in that HH∝1 yielded a strong interstrand crosslink, while the other two hammerheads did not. Sequence analysis of each labeled strand

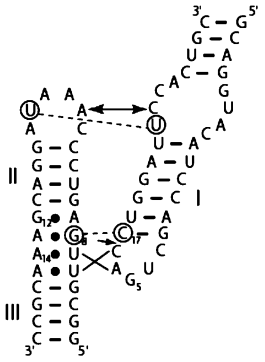

FIGURE 4: Sequence of a trans-cleaving variant of the native *S. mansoni* hammerhead ribozyme whose structure is stabilized by loop−loop interactions (double-headed arrow). This construct, without nucleotide analogues but using 254 nm UV light as described in the Materials and Methods, yielded two strong crosslinked bands. Each strand of each crosslink was sequenced as shown in Figure 3, and the crosslinks are indicated by circled nucleotides and dotted lines. The G8 to C1.1 crosslink is essentially the same as that obtained in HH∝1 with 254 nm light and also the reciprocal crosslinks obtained in HH16 with 312 nm light and crosslinking agents. The U-U crosslink between the two loops supports the hypothesis that the two loops form stabilizing tertiary interactions that keep domains 1 and 2 close together.

in the crosslinked species showed that the crosslink joined G8 on the short strand of HH∝1 to U1.1 on the long, cleavable strand. This crosslink is consistent with those obtained in HH16 using 6-S-dG8 and using 6-S-dG1.1, but in HH∝1, residues G8 and U1.1 evidently stack closely enough upon one another to yield a strong, spontaneous crosslink product upon 254 nm UV irradiation. HH∝1 has a cleavage rate approximately 10-fold faster than that of HH16, and it has been shown that a helix I sequence with a pyrimidine residue at position 1.1 both correlates with the faster cleavage rate (independent of strand connectivity) (*29*) and seems to position stems 1 and 2 at a more acute angle than a helix I sequence with a purine at position 1.1 (*4*, *20*).

A trans-acting version of the native *Schistosoma mansoni* hammerhead ribozyme (*30*, *31*) was also tested for photocrosslinking with 254 nm UV light. This construct yielded two strong crosslinks. Sequence analysis showed that one of the crosslinks connected G8 to C1.1, analogous to the G8 to U1.1 crosslink in HH∝1. The second crosslink joined a uridine in the internal loop of stem I to another uridine in loop II (Figure 4). This stacking relationship supports the putative "kissing loop" interaction, which is postulated to stabilize the folding of the natural ribozyme and facilitate its activity at physiological conditions.

A $Co(NH_3)_6^{3+}$-Mediated Crosslink between G8 and the Substrate Cleavage Site Retains Catalytic Activity. All of the photocrosslinks described in the preceding sections were tested for retention of cleavage activity. Isolated interstrand crosslinks were incubated at 37 °C in pH 8 buffer plus 20−30 mM $MgCl_2$ for 2−3 h and analyzed by denaturing gel electrophoresis. None of them demonstrated definitive cleavage activity. This is consistent with previous observations that crosslinks between stems I and II of the hammerhead ribozyme permitted the complex to retain cleavage (and ligation) activity (*32*), but crosslinks involving core positions of the ribozyme were inactive. This makes it difficult to evaluate the structural information generated by core crosslinks, because they could represent misfolded structures, folded

structures not yet accessing the transition state, or fully active structures, and retention of catalytic activity is the best basis for identifying stacking relationships formed in the active cleavage conformation.

$Co(NH_3)_6^{3+}$ is an exchange-inert trivalent metal complex that has been used as an analogue of hexahydrated magnesium ions in RNA studies. $Co(NH_3)_6^{3+}$ mediates folding and cleavage activity of the hairpin ribozyme (*33*−*35*), but at comparable concentrations, it fails to support activity of the hammerhead and it inhibits its Mg^{2+}-dependent cleavage (*36*). However, Bartel and colleagues (*7*) reported that concentrations of $Co(NH_3)_6^{3+}$ of 10 mM or greater could mediate hammerhead activity, albeit at reduced rates compared to those observed in magnesium.

$Co(NH_3)_6^{3+}$ absorbs ultraviolet light in the 300−400 nm range, and it can mediate photocrosslinking of unmodified RNA strands. For the hairpin ribozyme, exposure to 312 nm UV light in the presence of $Co(NH_3)_6^{3+}$ results in the formation of two prominent photocrosslinks that retain catalytic activity when reassembled and incubated. One of these crosslinks connects the hairpin residue G8 to A-1 of the substrate, the nucleotide just 5′ of the cleavable linkage (*12*). This crosslink is active although the Watson−Crick face of G8 is an important participant in catalysis. The G8 to A-1 stacking implied by this crosslink was later confirmed by the crystal structure of the hairpin ribozyme (*10*).

When the HH∝1 ribozyme was incubated with 10 mM $Co(NH_3)_6^{3+}$ and exposed to 312 nm UV light, it showed slow cleavage activity and yielded two strong photocrosslinks. One was proven to be from the end of a helix, but the other could be shown by sequence analysis to involve G8 from the short strand of HH∝1 (Figure 5A). Sequencing of the long strand showed cutoffs around C17 and U1.1 and also the presence of a cleavage product band from reversal of the crosslink (Figure 5B). When this crosslinked species, 5′-labeled on the long or short strand, was incubated in the presence of 30 mM $MgCl_2$ or 1 M $LiCl_2$, it yielded a band with mobility consistent with a cleaved but still crosslinked species. The increase in mobility is consistent with removal of the 3′-cleavage product (five nucleotides in length) from the crosslinked species, whether 5′-labeled on the long or short strand (Figure 5C). This implies that the active crosslinked species connects G8 on the short strand of HH∝1 to C17, just 5′ of the cleavage site on the long, cleavable strand (If the crosslink target were 3′ of the cleavable linkage, then cleavage of the crosslinked species would have yielded a normal long-strand cleavage product rather than the bands observed). Production of the cleaved crosslink band was dependent on the presence of $MgCl_2$ or LiCl and on the presence of a 2′-OH on the residue at the cleavage site. Crosslinks made with noncleavable 2′-deoxy-C17 in the long strand fail to give the putative "cleaved crosslink" band, whether incubated in the presence or absence of $MgCl_2$ (Figure 5C).

DISCUSSION

These experiments were designed to ask whether residues of the hammerhead ribozyme enter into intimate stacking relationships with the substrate nucleotides at any point during folding or catalysis. The efforts were initiated with nucleotide analogues substituted for G5, G8, and G12 for three reasons: (1) the ability of the ribozyme to function in high monovalent ion concentrations suggests that a general acid−base mechanism might be utilized; (2) the steep pH-rate profile of the hammerhead cleavage reaction implies that a functional group with a high pK_a might play an essential role in catalysis, and because guanosine has a high N1 pK_a (∼9.6), these three essential Gs are possible candidates; and (3) in the hairpin ribozyme (isolated from the opposite strand of the same satellite RNA of the Tobacco Ringspot Virus in which the hammerhead was identified), there is an essential guanosine involved in catalysis, and this G8 can be photocrosslinked to the adenosine 5′ of the cleavable linkage (*12*). The resulting crosslink retains the ability to catalyze cleavage when supplied with the missing third RNA strand and metal ions, showing that it represents an active conformation of the hairpin ribozyme. Thus, if the hammerhead reaction mechanism is related in some fashion to that of the hairpin, it might position one or more guanosines close to the cleavable bond.

It is notable that nearly all of the crosslinking agents used in this study yielded either no crosslinked products or a single band whose analysis revealed a single target. This suggests that the crosslinks do not represent random samplings of conformational space. Also, all of these crosslinks were dependent upon the presence of magnesium. Two of the crosslinks more consistent with the crystal structure, 4-S-dU4 to C17 and 4-S-dU7 to C17, could be obtained in low concentrations of magnesium (1 mM and lower), but the crosslinks from analogues at most other positions including 5, 8, and 12 required 10−30 mM $MgCl_2$ for optimal yields (data not shown). In backbone protection studies of the hammerhead, Hampel and Burke (*21*) found that HH16 could be folded, with a K_d^{Mg} of 1.1 ± 0.1 mM, into a shape resembling that of the crystal structures but slightly more compact. However, the cleavage activity of the same ribozyme showed a K_d^{Mg} of 20.7 ± 2.3 mM. Thus, crosslinks representative of an active conformation might be expected to require fairly high Mg^{2+} concentrations.

The most interesting of the latter class of crosslinks are the multiple examples implying stacking relationships between G12 and C17 and between G8 and G1.1, plus the more puzzling crosslink between G5 and G1.1. The first crosslinks involving G8 and G5 were somewhat suspect, because the 2′-deoxyribose of 6-S-dG is detrimental to ribozyme folding and function at those two positions (*16*, *22*). However, the G5 to G1.1 crosslink was reproduced using 8-bromo-G5 (ribo), and the G8 crosslink to the 1.1 position was obtained in two different constructs containing pyrimidines at 1.1, with short wavelength UV light and no crosslinking agent. A reciprocal crosslink was also obtained from 6-S-dG1.1 in HH16, targeting G8.

Thus, the evidence consistently suggests that C17 and G1.1 (or U or C1.1) closely approach and stack upon G12 and G8 in the tandem G−A mismatch motif of domain 2. The overall pattern of crosslinking could possibly represent a "folding pathway" for C17 and N1.1 during both the basic fold and accession of the transition state. The crosslinks of C17 to analogues of U4 and U7 might represent stacking relationships in the "resting" conformation, close to the status of the crystal structure. Then, C17 and N1.1 might flip outward from their nearly A-form configuration and interact

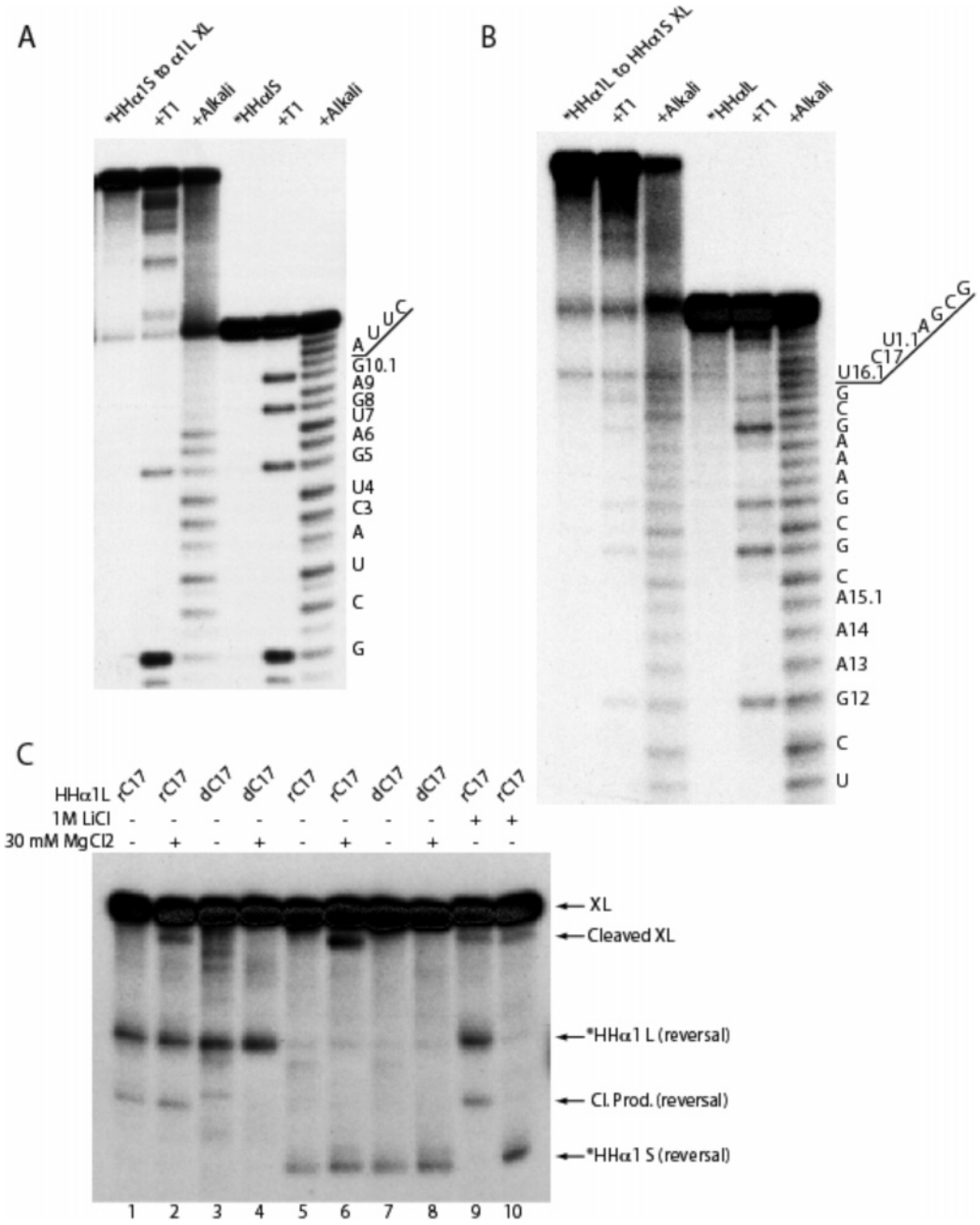

FIGURE 5: Analysis of crosslink targets and retention of cleavage activity for a crosslink in HH∝1 mediated by 10 mM $Co(NH_3)_6^{3+}$ and 312 nm light. The crosslink was obtained and analyzed as described in the Materials and Methods. (A) Sequence of the end-labeled short strand of HH∝1 and the crosslink, as described in Figure 3, showing that the crosslink targets G8. (B) Sequence of the end-labeled long strand of HH∝1 and the $Co(NH_3)_6^{3+}$ crosslink. The pattern in the Alkali lane is readable up to C17, but the crosslink yields a band at C17 as a reversal product (absent if the dC17 long strand is used and, thus, likely the actual cleavage product). Thus, the crosslink can be localized to C17, U1.1, or perhaps both. (C) Assay for cleavage activity of the HH∝1 crosslink mediated by $Co(NH_3)_6^{3+}$. Crosslinks were produced using the cleavable or noncleavable (dC17) long strand of HH∝1, with either the long or short strand 5′-end labeled. Crosslinks were incubated for 2.5 h with or without 30 mM $MgCl_2$ or with 1 M LiCl, as described in the Materials and Methods. In lanes 1−4 and 9, the HH∝1 long strand was end-labeled; in lanes 5−8 and 10, the short strand was labeled. Ribozyme cleavage 3′ of C17 removes the 3′ cleavage product (5 nt) from each labeled version of the crosslink, leaving cleaved products still crosslinked, containing all but 5 nucleotides of the HH∝1 long strand. The cleaved crosslink band is not produced in reactions incubated without magnesium (or LiCl) nor is it produced from crosslinks containing dC17, with or without magnesium (Lane 3 shows accidental nuclease degradation but no band corresponding to cleaved crosslink). The pattern implies that the portion of crosslink connecting G8 to C17 is catalytically active.

with domain 2, as implied by the G12 and G8 crosslinks. Flipping C17 out of its helix was suggested by Pley et al. (*8*) as one possibility for realigning the cleavable bond to render it more suitable for an S_N2 reaction. Such a movement of domain 1 into domain 2 would also be consistent with the implications of metal rescue experiments from Herschlag and colleagues (*37*), which suggested that the cleavable bond might be interacting with the same metal ion coordinating to the phosphate of A9 and N7 of G10.1.

If C17 and N1.1 of the substrate change orientation and move into close stacking relationships with the Gs of the tandem G−A mismatch motif in domain 2, then some change might be expected in the U-turn motif involving residues C3, U4, G5, and A6 of the ribozyme. The only relevant

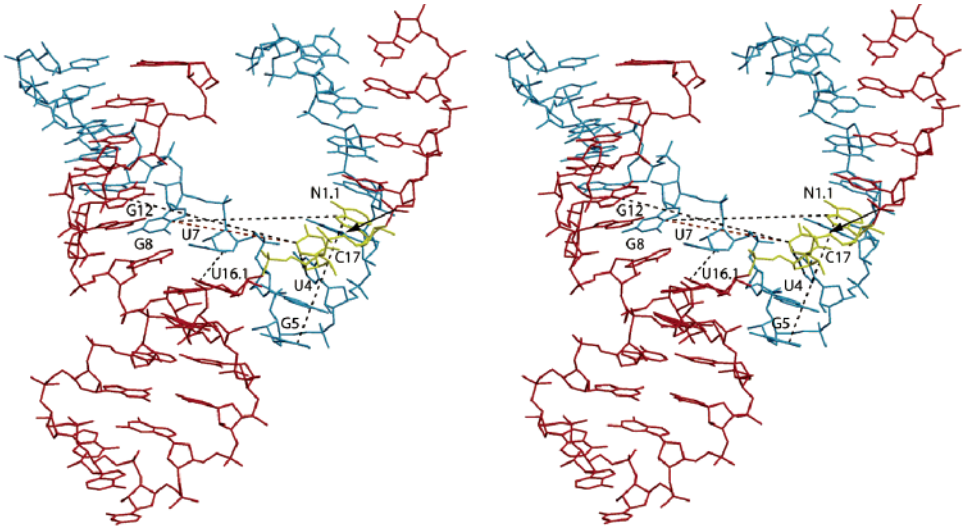

FIGURE 6: Stereo crystal structure model of the hammerhead ribozyme (from ref *9*) with photocrosslinks from this work presented as dotted lines. The red dotted line shows the $Co(NH_3)_6^{3+}$-induced catalytically active crosslink between G8 and C17. Distances between crosslinked bases, as measured in the crystal structure, are as follows: G12−C17, 15.6 Å; G8−N1.1, 15.7 Å; G5−N1.1, 12.4 Å; G8−C17 (active), 11.5 Å; U4−C17, 6.4 Å; and U16.1−U7, 3.8 Å.

information from these studies issues from the reproducible but somewhat puzzling crosslinks from 6-S-dG5 and 8-Br-G5 to G1.1 in the substrate. Because G8 also crosslinks to position 1.1, these findings, if not artifactual, imply formation of a complex, crowded set of interactions at the active site. This might at least begin to provide some explanation for the vast difference between the functional importance of G5 (*4*) and its unimpressive, solvent-exposed position in the crystal structures (*8*, *9*). Uhlenbeck and colleagues (*38*) carried out steric hindrance modification studies on the hammerhead, placing bulky groups onto the 2′ positions of residues in the ribozyme. They found that modifications that could theoretically be accommodated in the crystal structure interfered with the ribozyme function when placed at position 1.1 of the substrate, C3 and U4 of the U-turn motif, and also G12, A14, and A15.1 of domain 2. They concluded that the cleavage reaction requires conformational changes involving both domains 1 and 2 of the hammerhead, as implied by the crosslinking results reported here.

The isolation of an active $Co(NH_3)_6^{3+}$-induced crosslink between G8 and C17 in HH∝1 helps to validate the hypothesis that stacking of C17 and N1.1 of the substrate with G8 and G12 in domain 2 may be a necessary step in forming the catalytic conformation of the hammerhead. Cobalt hexaammine mediates cleavage by the hammerhead ribozyme only at moderately high concentrations (10 mM and above) and at rates slower than those observed in Mg^{2+} (*7*). It was used in these experiments because of its proven value as an inducer of photocrosslinks in the hairpin ribozyme. $Co(NH_3)_6^{3+}$ mediates nearly wild-type levels of activity in the hairpin ribozyme (*33*−*35*). The metal complex is orange in color and has a broad absorption peak in the long-wavelength UV range between 300 and 400 nm. It coordinates to nucleic acids in a manner similar but not identical to that of hexahydrated magnesium (*39*). Because of its absorption of UV light, $Co(NH_3)_6^{3+}$ can mediate strong photocrosslinks of unmodified RNA structures when exposed to 312 nm light (Pecore, Heckman, Lambert, and Burke, unpublished results) (*12*). In the hairpin ribozyme, it induces a crosslink between G8 in loop A (similarity to hammerhead numbering is coincidental) of the ribozyme and residue A-1 of the substrate, immediately 5′ of the cleavable linkage. This crosslinked species retains cleavage activity, which is remarkable, in view of the evidence that the Watson−Crick face of G8 has an important role in hairpin catalysis (*12*). Many photocrosslinking reactions result in chemical rearrangements of the bases involved (*28*). If one of those bases should be an important participant in reaction chemistry, then the crosslinked species could be rendered inactive, not by its geometry, but by disruption of functional groups needed for catalysis. The $Co(NH_3)_6^{3+}$-mediated hairpin crosslink of G8 to A-1 may be a simpler single covalent linkage (possibly from N7) (Pecore and Burke, unpublished results) that joins the bases without serious disruption.

The active hammerhead G8-C17 crosslink may represent a structural relationship similar to that in the hairpin, where the guanosine residue approaches the cleavable bond and participates in the chemistry of cleavage. G8 in the hammerhead may also play some role in the cleavage reaction. Efforts are underway to refine these observations and to generate molecular models of the putative active structure implied by the findings. Biochemical experiments based on this work and reported elsewhere have investigated the relationship between the pH-rate profile of the hammerhead cleavage reaction and the N1 pK_a values of nucleotide analogues placed at positions 5, 8, and 12 (Han and Burke, unpublished results). Results of these studies provide evidence that G8 and G12 may affect reaction chemistry directly, while the influence of G5 is exerted in folding rather than chemistry.

ACKNOWLEDGMENT

We thank Robert Pinard, Kenneth Hampel, Christina Pecore, and Joonhee Han for helpful discussions and insights. We thank Michael Fay for synthesis of RNA and Anne MacLeod for manuscript preparation.

REFERENCES

1. Winkler, W. C., Nahvi, A., Roth, A., Collins, J. A., and Breaker, R. R. (2004) Control of gene expression by a natural metabolite-responsive ribozyme, *Nature 428*, 281−286.

2. van Tol, H., Buzayan, J. M., Feldstein, P. A., Eckstein, F., and Bruening, G. (1990) Two autolytic processing reactions of a satellite RNA proceed with inversion of configuration, *Nucleic Acids Res. 18*, 1971−1975.
3. Slim, G., and Gait, M. J. (1991) Configurationally defined phosphorothioate-containing oligoribonucleotides in the study of the mechanism of cleavage of hammerhead ribozymes, *Nucleic Acids Res. 19*, 1183−1188.
4. Wedekind, J. E., and McKay, D. B. (1998) Crystallographic structures of the hammerhead ribozyme: Relationship to ribozyme folding and catalysis, *Annu. Rev. Biophys. Biomol. Struct. 27*, 475−502.
5. Murray, J. B., Seyhan, A. A., Walter, N. G., Burke, J. M., and Scott, W. G. (1998) The hammerhead, hairpin, and VS ribozymes are catalytically proficient in monovalent cations alone, *Chem. Biol. 5*, 587−595.
6. O'Rear, J. L., Wang, S., Feig, A. L., Beigelman, L., Uhlenbeck, O. C., and Herschlag, D. (2001) Comparison of the hammerhead cleavage reactions stimulated by monovalent and divalent cations, *RNA 7*, 537−545.
7. Curtis, E. A., and Bartel, D. P. (2001) The hammerhead cleavage reaction in monovalent cations, *RNA 7*, 546−552.
8. Pley, H. W., Flaherty, K. M., and McKay, D. B. (1994) Three-dimensional structure of a hammerhead ribozyme, *Nature 372*, 68−74.
9. Scott, W. G., Finch, J. T., and Klug, A. (1995) The crystal structure of an all-RNA hammerhead ribozyme: A proposed mechanism for RNA catalytic cleavage, *Cell 81*, 991−1002.
10. Rupert, P. B., and Ferre-D'Amare, A. R. (2001) Crystal structure of a hairpin ribozyme−inhibitor complex with implications for catalysis, *Nature 410*, 780−786.
11. Ferre-D'Amare, A. R., Zhou, K., and Doudna, J. A. (1998) Crystal structure of a hepatitis δ virus ribozyme, *Nature 395*, 567−574.
12. Pinard, R., Hampel, K. J., Heckman, J. E., Lambert, D., Chan, P. A., Major, F., and Burke, J. M. (2001) Functional involvement of G8 in the hairpin ribozyme cleavage mechanism, *EMBO J. 20*, 6434−6442.
13. Nakano, S., Chadalavada, D. M., and Bevilacqua, P. C. (2000) General acid−base catalysis in the mechanism of a hepatitis δ virus ribozyme, *Science 287*, 1493−1497.
14. Perrotta, A. T., Shih, I., and Been, M. D. (1999) Imidazole rescue of a cytosine mutation in a self-cleaving ribozyme, *Science 286*, 123−126.
15. Costa, M., and Michel, F. (1997) Rules for RNA recognition of GNRA tetraloops deduced by *in vitro* selection: Comparison with *in vivo* evolution, *EMBO J. 16*, 3289−3302.
16. McKay, D. B. (1996) Structure and function of the hammerhead ribozyme: An unfinished story, *RNA 2*, 395−403.
17. Quigley, G. J., and Rich, A. (1976) Structural domains of transfer RNA molecules, *Science 194*, 796−806.
18. Kuimelis, R. G., and McLaughlin, L. W. (1996) *Nucleic Acids and Molecular Biology*, Vol. 10, Springer-Verlag, Berlin, Germany.
19. Bassi, G. S., Murchie, A. I., Walter, F., Clegg, R. M., and Lilley, D. M. (1997) Ion-induced folding of the hammerhead ribozyme: A fluorescence resonance energy transfer study, *EMBO J. 16*, 7481−7489.
20. Amiri, K. M., and Hagerman, P. J. (1996) The global conformation of an active hammerhead RNA during the process of self-cleavage, *J. Mol. Biol. 261*, 125−134.
21. Hampel, K. J., and Burke, J. M. (2003) Solvent protection of the hammerhead ribozyme in the ground state: Evidence for a cation-assisted conformational change leading to catalysis, *Biochemistry 42*, 4421−4429.
22. Bassi, G. S., Murchie, A. I., and Lilley, D. M. (1996) The ion-induced folding of the hammerhead ribozyme: Core sequence changes that perturb folding into the active conformation, *RNA 2*, 756−768.
23. Dunham, C. M., Murray, J. B., and Scott, W. G. (2003) A helical twist-induced conformational switch activates cleavage in the hammerhead ribozyme, *J. Mol. Biol. 332*, 327−336.
24. Han, J., and Burke, J. M. (2004) Model for general acid−base catalysis by the hammerhead ribozyme: pH-activity relationships of G8 and G12 variants at the putative active site, manuscript submitted.
25. Walter, N. G., Yang, N., and Burke, J. M. (2000) Probing non-selective cation binding in the hairpin ribozyme with Tb^{III}, *J. Mol. Biol. 298*, 539−555.
26. Lockard, R. E., Alzner-Deweerd, B., Heckman, J. E., MacGee, J., Tabor, M. W., and RajBhandary, U. L. (1978) Sequence analysis of 5′[^{32}P] labeled mRNA and tRNA using polyacrylamide gel electrophoresis, *Nucleic Acids Res. 5*, 37−56.
27. Pinard, R., Heckman, J. E., and Burke, J. M. (1999) Alignment of the two domains of the hairpin ribozyme−substrate complex defined by interdomain photoaffinity crosslinking, *J. Mol. Biol. 287*, 239−251.
28. Favre, A., Saintome, C., Fourrey, J. L., Clivio, P., and Laugaa, P. (1998) Thionucleobases as intrinsic photoaffinity probes of nucleic acid structure and nucleic acid−protein interactions, *J. Photochem. Photobiol., B 42*, 109−124.
29. Clouet-d'Orval, B., and Uhlenbeck, O. C. (1997) Hammerhead ribozymes with a faster cleavage rate, *Biochemistry 36*, 9087−9092.
30. Canny, M. D., Jucker, F. M., Kellogg, E., Khvorova, A., Jayasena, S. D., and Pardi, A. (2004) Fast cleavage kinetics of a natural hammerhead ribozyme, *J. Am. Chem. Soc. 126*, 10848−10849.
31. Penedo, J. C., Wilson, T. J., Jayasena, S. D., Khvorova, A., and Lilley, D. M. (2004) Folding of the natural hammerhead ribozyme is enhanced by interaction of auxiliary elements, *RNA 10*, 880−888.
32. Stage-Zimmermann, T. K., and Uhlenbeck, O. C. (2001) A covalent crosslink converts the hammerhead ribozyme from a ribonuclease to an RNA ligase, *Nat. Struct. Biol. 8*, 863−867.
33. Hampel, A., and Cowan, J. A. (1997) A unique mechanism for RNA catalysis: The role of metal cofactors in hairpin ribozyme cleavage, *Chem. Biol. 4*, 513−517.
34. Nesbitt, S., Hegg, L. A., and Fedor, M. J. (1997) An unusual pH-independent and metal-ion-independent mechanism for hairpin ribozyme catalysis, *Chem. Biol. 4*, 619−630.
35. Young, K. J., Gill, F., and Grasby, J. A. (1997) Metal ions play a passive role in the hairpin ribozyme catalysed reaction, *Nucleic Acids Res. 25*, 3760−3766.
36. Horton, T. E., and DeRose, V. J. (2000) Cobalt hexammine inhibition of the hammerhead ribozyme, *Biochemistry 39*, 11408−11416.
37. Peracchi, A., Beigelman, L., Scott, E. C., Uhlenbeck, O. C., and Herschlag, D. (1997) Involvement of a specific metal ion in the transition of the hammerhead ribozyme to its catalytic conformation, *J. Biol. Chem. 272*, 26822−26826.
38. Blount, K. F., Grover, N. L., Mokler, V., Beigelman, L., and Uhlenbeck, O. C. (2002) Steric interference modification of the hammerhead ribozyme, *Chem. Biol. 9*, 1009−1016.
39. Gessner, R. V., Quigley, G. J., Wang, A. H., van der Marel, G. A., van Boom, J. H., and Rich, A. (1985) Structural basis for stabilization of Z-DNA by cobalt hexaammine and magnesium cations, *Biochemistry 24*, 237−240.

BI047858B